

Ion-Complexation-Induced Changes in the Interaction Parameter and the Chain Conformation of PS-*b*-PMMA Copolymers

Jia-Yu Wang, Wei Chen, and Thomas P. Russell*

Department of Polymer Science and Engineering, University of Massachusetts, Amherst, Massachusetts 01003

Received March 31, 2008; Revised Manuscript Received April 30, 2008

ABSTRACT: Small-angle neutron scattering (SANS) was used to study the changes of segmental interactions and chain conformation due to the formation of lithium–PMMA complexes in polystyrene-*block*-poly(methyl methacrylate) (PS-*b*-PMMA) copolymers as a function of temperature and the percentage of carbonyl groups coordinated with lithium ions. χ_{effc} and statistical segmental length, σ , are derived from the SANS profiles of the copolymers with lithium–PMMA complexes in a disordered state by use of the correlation-hole scattering formalism described by Leibler. Fitting results show that both χ_{effc} and σ of PS and PMMA increase as the formation of lithium–PMMA complexes in PS-*b*-PMMA copolymers, and the degree of such increase depends on the concentration of lithium–PMMA complexes. In addition, χ_{effc} of the lithium-complexed PS-*b*-PMMA becomes less temperature-dependent due to the increase in χ_s and decrease in χ_H .

Introduction

Ion-complexed polymers have attracted much attention because they carry high ionic conductivity, stable electrochemical characteristics, and excellent mechanical properties.^{1–5} Transition metal ions confined in the microdomains of block copolymers (BCPs) can also be converted into the corresponding metallic nanoparticles by reduction reactions, providing a simple route for the incorporation of inorganic nanoparticles into BCP microdomains.^{6–9} Recent studies showed that the formation of ionic complexes in copolymers dramatically changed the phase behavior of BCPs that had strong coordination interactions with the metal ions, for example, BCPs with poly(ethylene oxide) (PEO) or poly(vinylpyridine) (PVP) blocks. Mayes and co-workers observed a significant increase in order-to-disorder transition temperature (ODT) in poly(methyl methacrylate)-*b*-poly(oligo oxyethylene methacrylate) (PMMA-*b*-POEM) copolymers by the complexation of lithium trifluoromethanesulfonate (LiCF₃SO₃) with the PEO side chains.⁴ Subsequently, Bates and co-workers reported a similar phenomenon of an increase in ODT and microdomain spacing in poly(styrene-*b*-isoprene-*b*-ethylene oxide) (PS-*b*-PI-*b*-PEO) and poly(isoprene-*b*-styrene-*b*-ethylene oxide) (PI-*b*-PS-*b*-PEO) triblock copolymers complexed with lithium perchlorate (LiClO₄). They proposed that an effective interaction parameter, χ_{effc} , increased with the formation of lithium–PEO complexes.^{10,11} An increase in ODT and microdomain spacing was also observed in cadmium-complexed PS-*b*-P2VP copolymers by Kim et al., but the authors argued that the increase arose from the change of P2VP chain conformation due to the coordination of P2VP with cadmium ions, instead of an increase in χ_{effc} .¹²

More recently, we found an increase in the microdomain spacing and ordering in PS-*b*-PMMA copolymers as a consequence of the formation of lithium–PMMA complexes by the coordination of lithium ions with carbonyl groups in PMMA blocks. In addition, the formation of ionic complexes induced a disorder-to-order transition and an order-to-order transition from spherical to cylindrical morphologies.^{13,14} These observations imply that χ_{effc} of lithium-complexed PS-*b*-PMMA may increase due to the formation of lithium–PMMA complexes, but it has not been determined quantitatively. Furthermore, it

remains unclear how the chain conformation changes. To understand the physical origin in the phase behavior induced by lithium–PMMA complexes, we investigated the effective interaction parameter, χ_{effc} , and the chain conformation of lithium-complexed PS-*b*-PMMA copolymers by small-angle neutron scattering (SANS) as a function of temperature and the percentage of carbonyl groups coordinated with lithium ions. In comparison to the neat PS-*b*-PMMA copolymer, χ_{effc} and the statistical segmental lengths, σ , of both PS and PMMA increased in the lithium-complexed PS-*b*-PMMA copolymers to an extent that depended on the percentage of carbonyl groups coordinated with lithium ions. In addition, the temperature dependence of χ_{effc} for the lithium-complexed PS-*b*-PMMA was weaker than that for the neat copolymer. These results confirm that the changes in phase behavior induced by lithium–PMMA complexes, such as OOT, DOT, the increased microdomain ordering, and microdomain spacing, originate from the integrated effect of the increase in segmental interactions and the change in chain conformation.

Experimental Section

A diblock copolymer comprised of a perdeuterated polystyrene (d-PS) and a normal poly(methyl methacrylate) (PMMA), with a total number-average molecular weight, M_n , of 28 kg/mol ($N = 282$) and a polydispersity $PDI = 1.06$ was synthesized by sequential living anionic polymerization. The M_n of d-PS was 15 kg/mol ($N = 143$) with a polydispersity of 1.03 as determined from size-exclusion chromatography. The total volume fraction of d-PS in the diblock copolymer, f , was 0.53.

The lithium-complexed d-PS-*b*-PMMA copolymer was prepared by mixing two solutions of lithium chloride (LiCl) in tetrahydrofuran (THF) and the copolymer in toluene at a given ratio with continuous stirring and moderate heating until most of THF was evaporated and the solutions became clear. Details about this process can be found in previous reports.^{14–16} The percentage of the carbonyl groups complexed with lithium ions was estimated by FT-IR. No significant change in FT-IR profiles was observed as a function of temperature (Figure S1 in the Supporting Information).

Samples for the small-angle neutron scattering (SANS) measurements were prepared by compression-molding a powder of the copolymer into 1.5 cm diameter disks with 0.5 mm thickness at 150 °C. The disks were then heated to 135 °C under vacuum for 2 weeks and 170 °C under vacuum for 4 h. Samples for analysis were placed into demountable titanium cells fitted with quartz

*To whom correspondence should be addressed: e-mail russell@mail.pse.umass.edu.

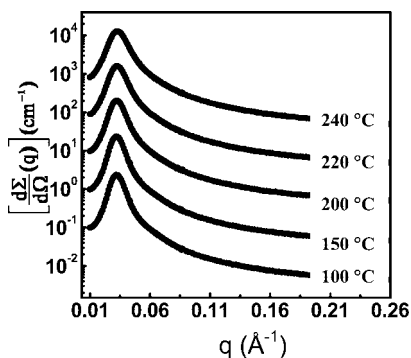


Figure 1. SANS profiles at various temperatures for the neat d-PS-*b*-PMMA copolymer. For clarity, SANS profiles are vertically shifted by a factor of 10.

windows. The entire assembly was mounted on a remote-controlled multisample block with a heating setup designed for the neutron spectrometer. Prior to each measurement, the samples were allowed 20 min to achieve thermal equilibrium. The temperature was monitored and controlled by a thermocouple located in close proximity to the samples. The temperature control was to within ± 1 °C at each temperature.

SANS measurements were performed at the Cold Neutron Research Facility at the National Institute of Standards and Technology on beamline NG-3 (see ref 17 for details of instrument design and operation). The wavelength of the neutron beam is 6 Å with $\Delta\lambda = 15\%$. Each measurement was performed in two different instrument configurations, characterized by nominal sample-to-detector distances of 2 and 5 m, resulting in a q range of 0.007–0.3 Å^{−1}. The scattered intensity was corrected for instrument dark current, empty cell scattering, and beam transmission to obtain the absolute neutron intensity by use of the available data reduction macros based on the IGOR Pro data analysis package.¹⁸ The incoherent scattering was set as one of the fitting parameters and was corrected for the fitting results.

Results and Discussion

SANS profiles ($I(q)$ vs $q = (4\pi \sin \theta)/\lambda$, where q is the scattering vector, 2θ is the scattering angle, and $I(q)$ is the absolute neutron scattering cross section) for the neat d-PS-*b*-PMMA copolymer obtained at five temperatures are shown in Figure 1. All the scattering profiles show a single, broad reflection arising from the correlation-hole scattering of a block copolymer in a disordered state.¹⁹ As the temperature increases from 100 to 240 °C, q_{max} values slightly shift from 0.0327 to 0.0336 Å^{−1}, $I(q_{\text{max}})$ decreases from 300 to 145 cm^{−1}, and the profiles broaden with the FWHM increasing from 0.0039 to 0.0058 Å^{−1}. The observations are consistent with the neat copolymer being in a disordered state.²⁰

Figure 2 shows the SANS profiles for the d-PS-*b*-PMMA copolymer with ~10% of carbonyl groups coordinated with lithium ions at the same temperatures as those for the neat copolymers. Similar to the case of the neat copolymer, all the scattering profiles have a single reflection. However, in contrast to those of the neat copolymer, q_{max} values shift $\sim 6.1\%$ to $q_{\text{max}} \sim 0.031$ Å^{−1}, $I(q_{\text{max}})$ increases moderately, and the scattering profiles sharpen. Since no higher order reflections appear, the changes in the shape and position of the scattering profiles are not sufficient to prove that the complexed copolymer has been driven into a microphase-separated state due to the increase in χ_{eff} . If the ion-complexed copolymer is in a disordered state, the experimental scattering profile should be described by the correlation-hole formalism described by Leibler.¹⁹ For the neat copolymer at 100 °C, the experimental and calculated profiles are consistent with the correlation-hole scattering (Figure S2A in the Supporting Information). However, for the copolymer

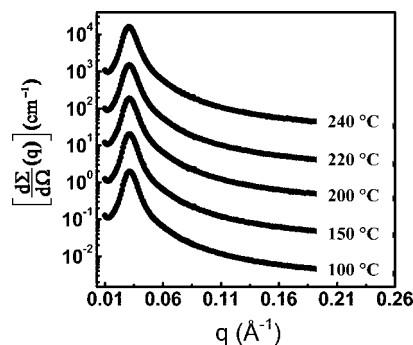


Figure 2. SANS profiles at various temperatures for the d-PS-*b*-PMMA copolymer with ~10% of carbonyl groups coordinate to lithium ions. For clarity, SANS profiles are vertically shifted by a factor of 10.

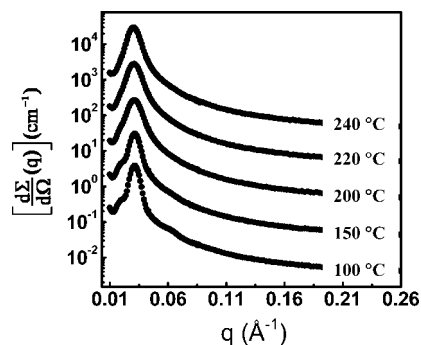


Figure 3. SANS profiles at various temperatures for the d-PS-*b*-PMMA copolymer with ~23% of carbonyl groups coordinate to lithium ions. For clarity, SANS profiles are vertically shifted by a factor of 10.

with ~10% of carbonyl groups coordinated to lithium ions at 100 °C, $I(q_{\text{max}})$ cannot be described by the simple correlation-hole argument (Figure S2B in the Supporting Information). Fredrickson et al.^{21–25} argued that close to the DOT composition fluctuations contribute significantly to the observed scattering, and the simple mean-field arguments do not work in this regime. Therefore, the mismatch between the experimental and calculated scattering profiles indicates that this ion-complexed copolymer at 100 °C may have been driven close to the phase boundary of the DOT but not fully microphase-separated since no higher order reflection is observed. In addition, over the entire experimental temperature range, gradual changes in q_{max} (from 0.0315 to 0.0313 Å^{−1}), $I(q_{\text{max}})$ (from 320 to 260 cm^{−1}), and the FWHM of the profiles (from 0.0036 to 0.0041 Å^{−1}) are observed.

As the percentage of carbonyl groups coordinated with lithium ions further increases to ~23%, the SANS profiles are significantly changed as shown in Figure 3. Below 200 °C, a very sharp peak at $q^* \sim 0.0310$ Å^{−1} with a second-order reflection at $2q^*$ demonstrates that the lamellar morphology is well developed in the ion-complexed copolymer, confirming that a DOT is induced by the ion complexation. With increasing temperature above 200 °C, the sharp reflection is replaced by a single, broad reflection that is characteristic of a block copolymer in a disordered state, indicating that temperature-induced ODT occurs. By increasing the temperature to 240 °C, no significant changes in q_{max} , $I(q_{\text{max}})$, and the FWHM are observed, similar to the copolymer with ~10% of carbonyl groups coordinated by lithium ions. The temperature dependence of χ for the neat PS-*b*-PMMA copolymer is weak ($\chi = (0.028 \pm 0.002) + (3.9 \pm 0.06)/T$).²⁰ As a result, the DOT/ODT can be observed only within a narrow molecular weight window, which is most difficult to control and to synthesize. Here, both the DOT and ODT are observed in the ion-complexed copolymer by control over temperature and concentration of lithium–PMMA com-

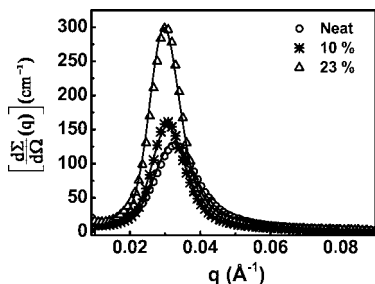


Figure 4. Comparison of the calculated (solid lines) and experimental (symbols) neutron scattering profiles at $T = 240\text{ }^{\circ}\text{C}$ for the neat d-PS-*b*-PMMA copolymer (○), the copolymers with $\sim 10\%$ (✱), and $\sim 23\%$ (Δ) of carbonyl groups coordinate to lithium ions. Here, $\chi = 0.03616$, 0.03647 , and 0.03702 were used in the calculations for the neat copolymer and the copolymers with $\sim 10\%$ and $\sim 23\%$ of carbonyl groups coordinate to lithium ions, respectively.

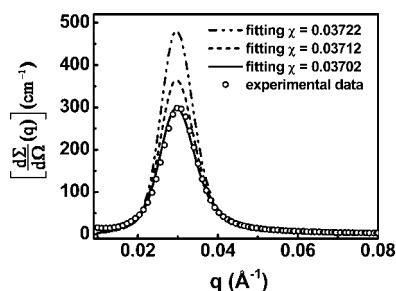


Figure 5. Comparison of the experimental neutron scattering profile (symbols) at $T = 240\text{ }^{\circ}\text{C}$ for the d-PS-*b*-PMMA copolymer with $\sim 23\%$ of carbonyl groups coordinate to lithium ions and calculated neutron scattering profiles (lines) where $\chi = 0.03702$, 0.03712 , and 0.03722 were used in the calculation.

plexes without varying the degree of polymerization, N , providing a simple way to tune the phase behavior of PS-*b*-PMMA copolymer.

For the neat copolymer and the copolymers with $\sim 10\%$ and $\sim 23\%$ of carbonyl groups coordinated to lithium ions, the SANS results suggest that all three samples are in the disordered state at temperature above $200\text{ }^{\circ}\text{C}$. This allows us to derive χ_{effc} and σ of each block as a function of temperature and the percentage of carbonyl groups coordinated with lithium ions from the correlation-hole scattering.¹⁹ The mathematical equations are well described in the earlier literature and not reproduced here.^{19,20,26} In principle, all the parameters for the calculation of the scattering profiles are known with the exception of the Flory–Huggins segmental interaction parameter, χ , and the statistical segment length, σ , of each component. The value of χ dictates the $I(q_{\text{max}})$ and the FWHM of the scattering profile, and the value of σ_i determines the position of q_{max} . Therefore, by varying χ and σ_i , the calculated scattering profiles can be fit to the experimental profiles. Figure 4 shows the comparisons between the experimental and calculated profiles for the neat copolymer and the copolymers with $\sim 10\%$ and $\sim 23\%$ of carbonyl groups coordinated to lithium ions at $240\text{ }^{\circ}\text{C}$. $\chi = 0.03616$, 0.03647 , and 0.03702 ; $\sigma_{\text{PS}} = 8.67$, 9.34 , and 9.41 ; and $\sigma_{\text{PMMA}} = 8.79$, 9.11 , and 9.60 were used for these three copolymers. The agreement in the shape and the position of q_{max} between theory and experiment is quite good over the entire scattering vector range at this temperature, confirming that the formation of lithium–PMMA complexes increases χ_{effc} and σ of each block, and the degree of the increase depends on the degree of complexation. The shape of the calculated scattering profile is quite sensitive to the value of χ . As shown in Figure 5, variation of χ by more than 0.0001 produced unacceptable fits to the experimental scattering profiles. Consequently, error limits of at most 0.0001 can be placed on the reported χ values.

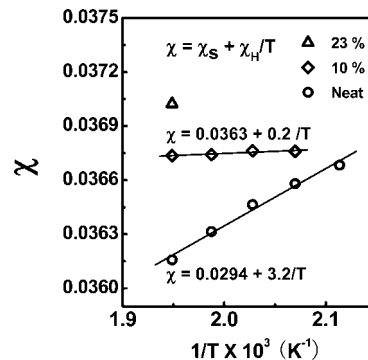


Figure 6. Segmental interaction parameter, χ , as a function of the reciprocal temperature for the neat d-PS-*b*-PMMA copolymer (○) and the copolymers with $\sim 10\%$ (✱) and $\sim 23\%$ (Δ) of carbonyl groups coordinate to lithium ions.

Figure 6 summarizes the fitting results of χ as a function of $1/T$ for the neat copolymer and the copolymer with $\sim 10\%$ and $\sim 23\%$ of carbonyl groups coordinated to lithium ions at temperature above $200\text{ }^{\circ}\text{C}$. The fitting parameters are listed in Table S1 in the Supporting Information. For the $\sim 10\%$ sample, a good fit can be achieved at temperatures of $210\text{--}240\text{ }^{\circ}\text{C}$. For the $\sim 23\%$ sample, only the scattering profile at $240\text{ }^{\circ}\text{C}$ can be reproduced. Below $240\text{ }^{\circ}\text{C}$ but above $200\text{ }^{\circ}\text{C}$, the discrepancies between the measured and predicted scattering profiles exist as shown in Figure S3. Over the entire temperature range in Figure 6, $\chi_{23\%} > \chi_{10\%} > \chi_{\text{neat}}$ is seen. For $\chi_{23\%}$ at temperature below $200\text{ }^{\circ}\text{C}$, the value should be much higher than 0.037 since the copolymer has been driven into the phase-separated state. But the exact value cannot be determined from the correlation-hole scattering. Though the effects of the composition fluctuations^{23–25} and polydispersity^{27–29} have not been taken into account in our study, the dependence of χ on temperature remains. Here, χ was found to vary as $1/T$ for both the neat copolymer and $\sim 10\%$ complexed copolymer, though the temperature dependence for the complexed copolymer was weaker. A linear least-squares fit to the data in Figure 6 gives $\chi_{\text{neat}} = (0.0294 \pm 0.0002) + (3.2 \pm 0.2)/T$, consistent with the previous result of $\chi = (0.028 \pm 0.002) + (3.9 \pm 0.6)/T$.²⁰ For the $\sim 10\%$ complexed copolymer, a similar fit gives $\chi_{\text{complexed}} = (0.0363 \pm 0.0001) + (0.20 \pm 0.07)/T$. Representing χ in terms of entropic, χ_s , and enthalpic, χ_H , χ can be described as $\chi = \chi_s + \chi_H/T$. A comparison of χ_{neat} and $\chi_{\text{complexed}}$ shows that the entropic contribution to χ for the complexed copolymer increased and the enthalpic contribution decreased, resulting in a nearly temperature-independent χ .

In conclusion, we have demonstrated the ion-complexation-induced changes in the segmental interaction parameter and the chain conformation of PS-*b*-PMMA copolymers. Both χ_{effc} and σ of PS and PMMA increase with the formation of lithium–PMMA complexes, and the extent of the increase depends on the concentration of lithium–PMMA complexes. In addition, because of an increase in χ_s and decrease in χ_H , χ_{effc} of the lithium-complexed PS-*b*-PMMA becomes less temperature-dependent.

Acknowledgment. This research was supported by the Department of Energy Basic Energy Science (DEFG0296ER45612) and the National Science Foundation-supported Material Research Science and Engineering Center at the University of Massachusetts, Amherst (DMR-0213695). We thank Dr. B. Hammouda for the useful discussion and Dr. S. Kline for the assistance with SANS measurements. This work utilized facilities supported in part by the National Science Foundation under Agreement No. DMR-0454672. We acknowledge the support of the National Institute of Standards and Technology, U.S. Department of Commerce, in providing the neutron research facilities used in this work.

Supporting Information Available: FT-IR absorption spectra, measured and calculated SANS profiles of the neat copolymer and copolymers with ~10% and 23% of carbonyl groups coordinate to lithium ions at different temperatures, and the temperature dependence of the fitting parameters for neat and lithium-complexed copolymers. This material is available free of charge via the Internet at <http://pubs.acs.org>.

References and Notes

- (1) MacGlashan, G. S.; Andreev, Y. G.; Bruce, P. G. *Nature (London)* **1999**, *398*, 792.
- (2) Gadjourova, Z.; Andreev, Y. G.; Tunstall, D. P.; Bruce, P. G. *Nature (London)* **2001**, *412*, 520.
- (3) Pereira, R. P.; Rocco, A. M.; Bielschowsky, C. E. *J. Phys. Chem. B* **2004**, *108*, 12677.
- (4) Ruzette, A. V.; Soo, P. P.; Sadoway, D. R.; Mayes, A. M. *J. Electrochem. Soc.* **2001**, *148*, A537.
- (5) Christie, A. M.; Lilley, S. J.; Staunton, E.; Andreev, Y. G.; Bruce, P. G. *Nature (London)* **2005**, *433*, 50.
- (6) Spatz, J. P.; Herzog, T.; Mossmer, S.; Ziemann, P.; Moller, M. *Adv. Mater.* **1999**, *11*, 149.
- (7) Breulmann, M.; Forster, S.; Antonietti, M. *Macromol. Chem. Phys.* **2000**, *201*, 204.
- (8) Sohn, B. H.; Yoo, S. I.; Seo, B. W.; Yun, S. H.; Park, S. M. *J. Am. Chem. Soc.* **2001**, *123*, 12734.
- (9) Glass, R.; Moller, M.; Spatz, J. P. *Nanotechnology* **2003**, *14*, 1153.
- (10) Epps, I., T. H.; Bailey, T. S.; Pham, H. D.; Bates, F. S. *Chem. Mater.* **2002**, *14*, 1706.
- (11) Epps, I., T. H.; Bailey, T. S.; Waletzko, R.; Bates, F. S. *Macromolecules* **2003**, *36*, 2873.
- (12) Lee, D. H.; Kim, H. Y.; Kim, J. K.; Huh, J.; Ryu, D. Y. *Macromolecules* **2006**, *39*, 2027.
- (13) Wang, J.-Y.; Leiston-Belanger, J. M.; Sievert, J. D.; Russell, T. P. *Macromolecules* **2006**, *39*, 8487.
- (14) Wang, J.-Y.; Chen, W.; Roy, C.; Sievert, J. D.; Russell, T. P. *Macromolecules* **2008**, *41*, 963.
- (15) Wang, J.-Y.; Chen, W.; Sievert, J. D.; Russell, T. P. *Langmuir* **2008**, *24*, 3545.
- (16) Wang, J.-Y.; Xu, T.; Leiston-Belanger, J. M.; Gupta, S.; Russell, T. P. *Phys. Rev. Lett.* **2006**, *96*, 128301.
- (17) Glinka, C. J.; Barker, J. G.; Hammouda, B.; Krueger, S.; Moyert, J. J.; Orts, W. J. *J. Appl. Crystallogr.* **1998**, *31*, 430.
- (18) Kline, S. R. *J. Appl. Crystallogr.* **2006**, *39*, 895.
- (19) Leibler, L. *Macromolecules* **1980**, *13*, 1602.
- (20) Russell, T. P.; Hjelm, R. P., Jr.; Seeger, P. A. *Macromolecules* **1990**, *23*, 890.
- (21) Bates, F. S.; Fredrickson, G. H. *Annu. Rev. Phys. Chem.* **1990**, *41*, 525.
- (22) Bates, F. S.; Rosedale, J. H.; Fredrickson, G. H. *J. Chem. Phys.* **1990**, *92*, 6255.
- (23) Fredrickson, G. H. *J. Chem. Phys.* **1986**, *85*, 5306.
- (24) Fredrickson, G. H.; Helfand, E. *J. Chem. Phys.* **1987**, *87*, 697.
- (25) Bates, F. S.; Rosedale, J. H.; Fredrickson, G. H.; Glinka, C. J. *Phys. Rev. Lett.* **1988**, *61*, 2229.
- (26) Ryu, D. Y.; Jeong, U.; Lee, D. H.; Kim, J.; Youn, H. S.; Kim, J. K. *Macromolecules* **2003**, *36*, 2894.
- (27) Leibler, L.; Benoit, H. *Polymer* **1981**, *22*, 195.
- (28) Bates, F. S.; Hartney, M. A. *Macromolecules* **1985**, *18*, 2487.
- (29) Owens, J. N.; Grancarz, I.; Koberstein, J. T.; Russell, T. P. *Macromolecules* **1989**, *22*, 3380.

MA800718Z